

Reactions of Electrons on the Surface of γ -Al₂O₃. A Pulse Radiolytic Study with 0.4 MeV Electrons

B. H. Milosavljevic and J. K. Thomas*

Department of Chemistry and Biochemistry, University of Notre Dame, Notre Dame, Indiana 46556-5670

Received: March 19, 2003

Radiolysis of γ -alumina produces electrons, e^- , and positive holes, h^+ . These species rapidly migrate to the surface to produce products of surface adsorbed compounds. The electrons are also trapped by surface OH groups giving rise to short-lived ($<10\ \mu\text{s}$) trapped electrons, e_t^- . Heating the γ -Al₂O₃ produces Lewis acid sites and decreases the OH content of the surface. Such material produces much lower yields of trapped electrons, as e^- then reacts predominantly with the Lewis acid sites. Hydrogen gas is produced on radiolysis of γ -Al₂O₃ via H atom formation from e^- . The H atoms may recombine, producing H₂, or react with surface adsorbed materials (e.g., pyrene) to produce H atom adducts. The basic radiation chemistry is similar to that observed in zeolites (but not SiO₂), where ionization predominates. These studies illustrate for the first time the production of electrons in a γ -Al₂O₃ surface and the consequent two-dimensional kinetics of these species on the surface.

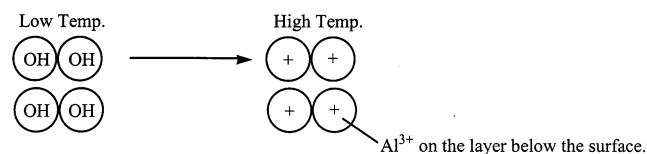
Introduction

In the areas of both material science and catalysis, radiation-induced reactions on solid surfaces are of particular interest. Much is available on radiation-induced reactions in the gas phase and in solution. However, only a few studies on radiation-induced effects at solid surfaces are available; this is particularly true of high-energy studies or radiolytic effects. Most studies in this area have been carried out via steady-state methods in silicas, aluminas, zeolites, and a few other metal oxides. In porous materials, the general concept that comes out of these studies is that energy deposited in the bulk of the solid is transferred to the surface, there creating chemistry.¹ The reactions studied include oxidation and decomposition of organic adsorbates and polymerization of various vinyl monomers.^{1–7} In general, reactive intermediates and reaction mechanisms involved in the chemical reactivity of the above solid systems are not clearly understood, except for some tentative propositions drawn from the analysis of final products. A detailed knowledge of the formation of transient intermediates and the structure–property relationship for these solids is essential in the design and preparation of specific catalysts.

Recent pulse radiolysis studies in porous silica⁸ and zeolites^{9,10} have illustrated well the varied and brilliant chemistry produced on radiolysis of these solids. The conclusion is that ionic species are produced in zeolites, positive holes, h^+ , and electrons, which are trapped in the metal clusters (e.g., on Na_4^{3+}). The h^+ and the electron can be readily transferred to species adsorbed to the surface of the zeolite, creating radical anions and cations as well as other products. By contrast, the radiolysis of porous SiO₂, while producing some ionic species such as electrons trapped in fortuitous surface OH configuration, nevertheless tends to produce radical chemistry, in particular, that of the H atom. The contrast between the two solid systems is quite marked.

As the zeolites are essentially silica-containing alumina (and counterions), it would be informative to study the pulse

radiolysis of alumina, to see where its chemistry lies with respect to zeolites and porous silica. Earlier photolytic studies of organic molecules adsorbed to porous γ alumina have indicated extensive ionic chemistry.^{11–14} Indeed, this increases on heat activation of the Al₂O₃, which produces acid sites,^{11–13,15,16} which are formed by elimination of H₂O from surface OH groups as indicated below.



The low-temperature sample contains a top layer of OH groups with a sublayer of Al atoms. Heating eliminates H₂O via the condensation of two OH groups. This leaves an incomplete surface layer of O atoms with halos and a sublayer of Al atoms. As the material is crystalline, the formal representation is a sublayer of Al³⁺ ions with a top surface of O²⁻ ions.

These studies tend to indicate that radiolysis of γ -Al₂O₃ should produce ionic chemistry. The studies below were undertaken to investigate this concept.

Experimental Section

The pulsed laser and Febetron systems have been described in earlier studies.^{8,11} Chemicals were obtained from Aldrich Chemical Co, and treated as described earlier.^{8,11}

Gamma alumina (HiQ-7219 CC) was a gift from the Alcoa Corporation. The material has a surface area of 200 m²/gm. A sample of γ -alumina was also obtained from Degussa Co., CAS No. 1344-284, surface area 100 m²/gm particle size 20 nm. In most cases, the material was irradiated as disks (0.01 cm thick), which were made by pressing the powder.^{8,11}

The irradiations were carried out either with Co⁶⁰ γ rays or with 2 ns pulses of 0.4 MeV electrons from a Febetron 706. The doses given to the samples were measured as follows: In

* Corresponding author. Fax: (574) 631-6652. E-mail: thomas.3@nd.edu.

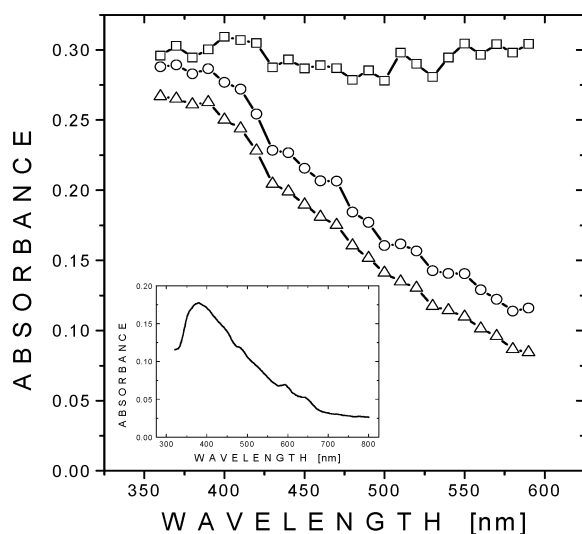


Figure 1. Pulse radiolysis data of γ -alumina obtained in a vacuum with a 2-ns pulse of 0.4 MeV electrons. Spectra taken immediately after the pulse (squares), at 1 (circles) and 9 μ s (triangles). Insert: Long-lived species at 77 K after γ irradiation with a dose of 8 kGy.

steady-state irradiation, doses to the samples were established by conventional methods using the Fricke dosimeter. In the pulsed studies, thin polymer films containing a radiochromic dye, FWT-60, from Far West Technologies, Goleta, CA, which have been demonstrated to be reliable even at the dose rate of 10^{13} Gy/sec,¹⁷ were used to measure the doses to the thin disks. In this dosimeter, irradiation causes an increased optical absorption in the polymer, which is measured at 605 nm.¹⁷

Results and Discussion

Pure γ - Al_2O_3 . Spectra and Kinetics. Figure 1 shows the spectrum of short-lived species obtained in the pulse radiolysis of γ alumina in a vacuum (<1 mTorr). The spectrum is essentially featureless, although the spectrum at longer times indicates a maximum below 400 nm. The maximum below 400 nm at 370 nm is confirmed by steady-state experiments at 77 K and irradiation with γ rays, as shown as an insert in Figure 1.

These spectra are consistent with an initial rapid decay followed by a much slower one. Typical data to illustrate this point are given in Figure 2a. It is noted that the rate of the initial sharp decay decreases with decreasing wavelength for 590–400 nm. A continuous smooth decrease is noted over this wavelength range and continuing to 360 nm. The rapid decay is removed by SF_6 and O_2 , while the long-lived decay is unaffected. The specificity of the reaction of SF_6 and O_2 indicates the short-lived decay is due to electrons.

The kinetics of the electron decay in Figure 2a are not well described by tunneling or any simple order. A good fit is obtained via an equation of the type

$$I = I_0 e^{-(kt)^\beta} \quad (1)$$

the best fit being with $\beta = 0.4$ (Table 1). In these calculations, the long-lived component shown in Figure 1, obtained at 8 μ s, was subtracted from the data. Such fits are shown in Figure 2b and it is noted that the kinetics are identical at two different doses. This type of kinetics and formulation is akin to geminate ion kinetics. In liquid systems, the exponent in time is (-0.6) and reflects on the geminate and three-dimensional nature of the system.¹⁸ In the present Al_2O_3 system, the geminate in

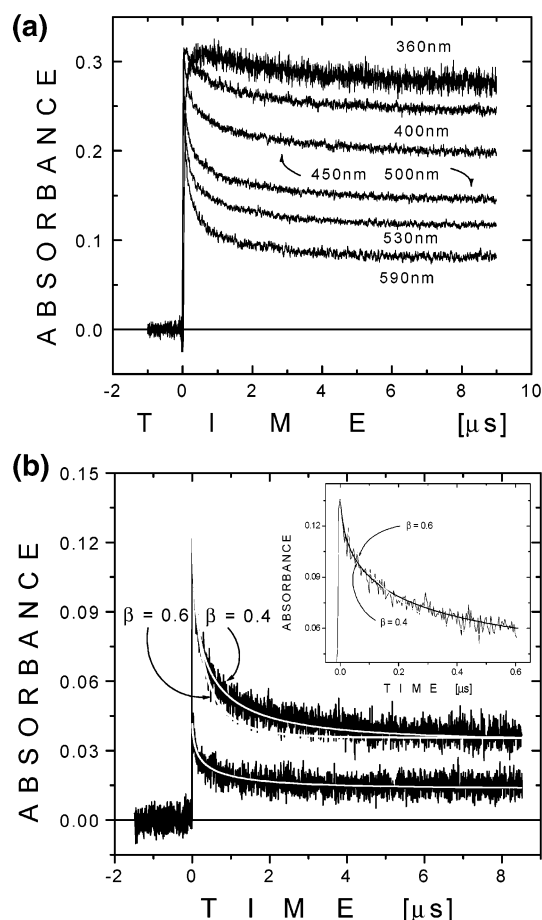
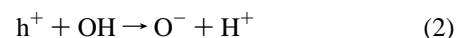


Figure 2. (a) Decay of e_t^- at various wavelength. (b) Fitting of e_t^- decay at 590 nm to $I = I_0 e^{-(kt)^\beta}$. Parameters obtained are listed in Table 1.

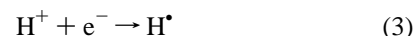
TABLE 1: Parameters Obtained in Fitting the Electron Decays by Eq 1

| sample | I_0 | k | β | long-lived component |
|------------------|-------|----------------------------------|---------|----------------------|
| higher intensity | 0.108 | $4.5 \times 10^6 \text{ s}^{-1}$ | 0.4 | 0.0355 |
| lower intensity | 0.035 | $4.5 \times 10^6 \text{ s}^{-1}$ | 0.4 | 0.0135 |

recombination occurs on a surface (i.e., in two dimensions). This is reflected in a reduced exponent in time (i.e., $t^{-0.4}$). Hence, the decays of Figure 2 are attributed to geminate ion decay of the trapped electron e_t^- with its concomitant positive ion. The surface of γ - Al_2O_3 is rich in OH groups, and it is suggested that positive hole h^+ , which is produced initially along with e^- rapidly decays to H^+ .



The observed geminate ion recombination is then



Heat Treatment. Prior heating of the γ alumina for 4 h at 450 $^\circ\text{C}$ eliminates the fast decay, while the long-lived decay is unaffected. This treatment decreases the surface OH content from $11.5 \times 10^{14}/\text{cm}^2$ to $4.6 \times 10^{14}/\text{cm}^2$, while increasing the Lewis acid site concentration from 0.8×10^{14} to $2.4 \times 10^{14}/\text{cm}^2$. These data suggest the following mechanism: Radiolysis produces e^- , and h^+ . The yield of these species is significant, $G > 1.0$ species/100 eV, as shown later in probe studies. Both e^- and h^+ move to the surface, as illustrated later by the

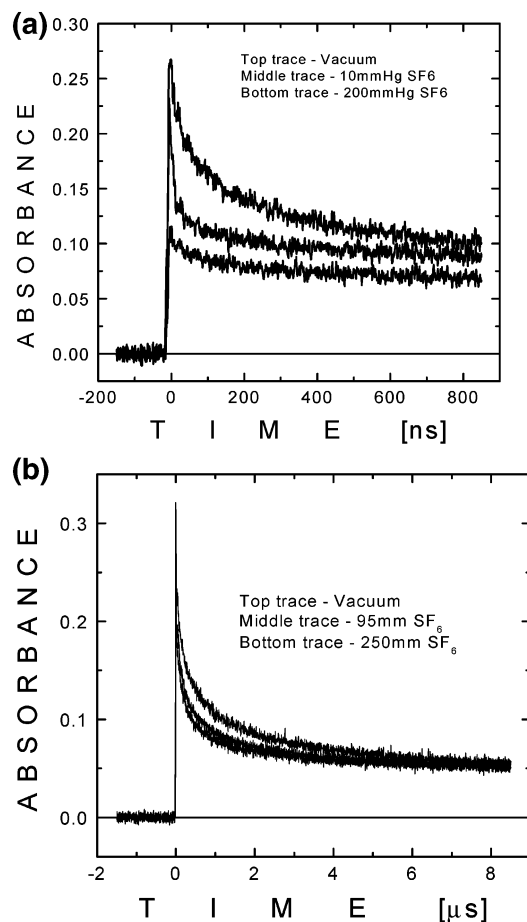
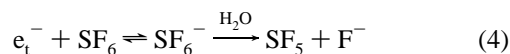


Figure 3. Effect of SF_6 on e_t^- decay at 590 nm, (a) with a surface layer of water, (b) dry surface.

formation of radical anions and cations of surface adsorbed molecules. The electrons are trapped in either fortuitous arrangements of surface OH groups or Lewis acid sites. The rapid decay of these electrons trapped by OH groups (e_t^-) is indicative of further reaction with counteranions and/or with Lewis acid sites. The varied rate of decay of e_t^- with wavelength indicates a wide variety of surface trapped electrons. The long-lived species remains an unknown at this time, what can be said about it is that it is a species produced in the bulk, as it does not react with any of the scavengers used.

Surface Reactions of Gases with e_t^- . It was indicated earlier that SF_6 and O_2 react rapidly with e_t^- . These reactions are markedly dependent on the surface water constant. Figure 3 shows the effect of various pressures of SF_6 on the decay of e_t^- on a dry surface and a surface with about 1 monolayer of water. It is noted that on the wet surface, as little as 10 Torr of SF_6 causes a rapid decay of e_t^- , while 200 Torr completely removes e_t^- , leaving only the long-lived component. In a dry system, 250 Torr of SF_6 only causes a factor of 2 increase in the rate of decay of e_t^- . A possible mechanism is given below and involves an initial equilibrium. The right side of which is done to separate ions by solvation by water molecules, as observed in



aqueous solution.¹⁹

Surface Adsorbed Reactants on γ - Al_2O_3 . Most arenes adsorb strongly to the γ Al_2O_3 surface via interaction with the

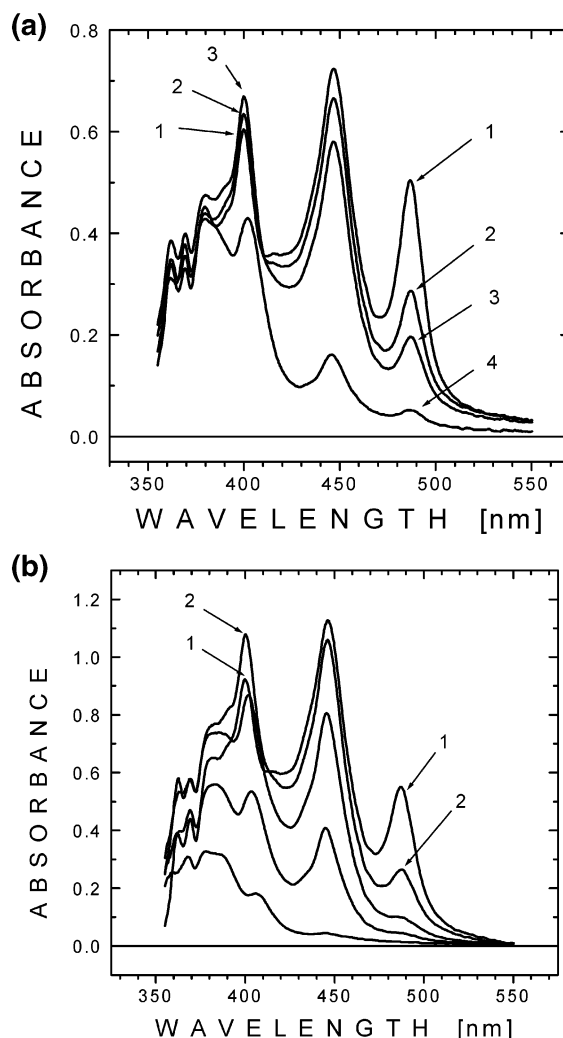


Figure 4. (a) Co^{60} γ irradiation of 10 $\mu\text{M/gm}$ pyrene on γ -alumina at 77 K. Spectra shown after annealing at room temperature for various periods of time. (b) As in (a), but γ - Al_2O_3 preheated for 2 h at 400 °C prior to loading with pyrene and irradiation.

surface OH groups (physisorption) and via the Lewis acid sites (chemisorption). The adsorbed probe reported here is pyrene, which we have used extensively in other surface studies, and is well characterized.^{8,9} Figure 4, parts a and b show the long-lived species produced on γ -radiolysis at 77 K of pyrene on Alcoa γ -alumina. In all cases, the pyrene anion, P^- , ($\lambda_{\text{max}} = 490$ nm), the pyrene cation, P^+ , ($\lambda_{\text{max}} = 447$ nm), and the H atom adduct, PH^* , ($\lambda_{\text{max}} = 400$ nm) are observed. In the unheated sample $G(\text{P}^-) = 1.0$, and $G(\text{P}^+) = 1.3$, and $G(\text{PH}^*) = 1.3$. On warming the sample, P^- and P^+ decay, while PH^* increases, with the decay of P^- being more rapid than that of P^+ . At sufficiently high temperatures, all pyrene species disappear, and only the long-lived bulk species of γ - Al_2O_3 is observed as in the case of pure γ Al_2O_3 . The adsorbed pyrene causes a significant decrease in the e_t^- absorption at 590 nm. This supports the assignment of this absorption to a trapped electron, as pyrene intercepts the e^- prior to trapping by the surface OH groups. The $G(\text{P}^-) = 1.0$ indicates that the original yield of e^- is much larger than $G = 1.0$. It is suggested that the formation of PH^* is via two processes: direct H atom addition to pyrene, as observed in SiO_2 ,⁸ and $\text{P}^- + \text{H}^+ \rightarrow \text{PH}^*$, as observed in liquid methanol²⁰ and poly(vinyl alcohol).²¹



TABLE 2: H₂ Gas Yields in the Radiolysis of Various Solids

| material | G(H ₂) molecule per 100 eV adsorbed |
|---------------|---|
| boehmite | 0.35 |
| γ-alumina | 0.54 |
| silica (60 Å) | 0.68 |
| zeolite Y* | 0.18 |

and a slower process via the interaction of P[−] with H⁺ formed in the original radiolysis process



followed by



These precise processes have been observed in methanol solution²⁰ and in polymer films.²¹

In the absence of surface adsorbed materials, H atoms are still formed as indicated by the large yield of hydrogen gas produced in radiolysis of γ-Al₂O₃, Table 2. The yield of H₂ on γ-Al₂O₃ is almost as large as that on SiO₂ and larger than that on zeolites, a solid that contains few OH groups. In SiO₂, it was shown⁸ that H₂ was produced via H atom recombination on the surface, this process competing with H atom reaction with surface adsorbed material. The similarity of the hydroxylated surfaces of SiO₂ and γ-Al₂O₃ and the similar yields of H₂ suggest that similar processes produce H₂ in both systems.

Conclusions

The radiolysis of γ-Al₂O₃ produces electrons and positive holes, which migrate to the surface of the solid, there producing chemical products of adsorbed molecules and also being trapped by surface OH groups. This chemistry is much akin to that observed in the radiolysis of zeolites but unlike that observed in porous Silica, where excitonic chemistry is prevalent.⁹ It is well known that excitation of amorphous SiO₂ leads to the formation of bound electron – hole pairs or excitons.²² These singlet excitons rapidly decay (250 fs) to triplet excitons.²³ The free excitons can be localized at surface OH causing a cleavage of the O–H band giving >SiO[•] and an H atom. In the case of zeolites and γ-alumina, the main role of excitation is ionization, and the subsequent surface chemistry directly reflects an ionic situation.

Acknowledgment. We wish to thank the National Science Foundation and the University of Notre Dame for support of this work.

References and Notes

- (1) Rabe, J. G.; Rabe, B.; Allen, A. O. *J. Am. Chem. Soc.* **1964**, *86*, 3887; *J. Phys. Chem.* **1966**, *70*, 1098.
- (2) Sutherland, J. W.; Allen, A., *J. Am. Chem. Soc.* **1961**, *83*, 1040. Abrams, L.; Allen, A. O. *J. Phys. Chem.* **1969**, *73*, 2741.
- (3) Hentz, R. R. *J. Phys. Chem.* **1962**, *66*, 1625. Hentz, R. R.; Wickenden, D. K. *J. Phys. Chem.* **1969**, *73*, 817.
- (4) Kohn, H. W. *J. Phys. Chem.* **1962**, *66*, 1185; *J. Phys. Chem.* **1964**, *68*, 3129.
- (5) Sagert, N. H.; Dyne, P. J. *Can. J. Chem.* **1967**, *45*, 615.
- (6) Shimada, M.; Nakamura, J.; Kusama, Y.; Udagawa, A.; Takehisa, M. *J. Appl. Polym. Sci.* **1982**, *27*, 1259.
- (7) Bruk, M. A.; Pavlov, G. G.; Isaeva, Yunitskaya, E. Ya *Eur. Polym. J.* **1986**, *22*, 169.
- (8) Zhang, G.; Mao, Y.; Thomas, J. K. *J. Phys. Chem.* **1997**, *101*, 7100.
- (9) Zhang, G.; Lui, X.; Thomas, J. K. *Rad Phys. Chem.* **1998**, *51*, 135.
- (10) Werst, D. W.; Han, P.; Trifunac, A. D. *Rad Phys. Chem.* **1998**, *51*, 255.
- (11) Pankasem, S.; Thomas, J. K. *J. Phys. Chem.* **1991**, *95*, 6990.
- (12) Pankasem, S.; Thomas, J. K. *J. Phys. Chem.* **1991**, *95*, 7385.
- (13) Pankasem, S.; Thomas, J. K. *Langmuir* **1992**, *8*, 501.
- (14) Beck, G.; Thomas, J. K. *Chem. Phys. Lett.* **1983**, *94*, 553.
- (15) Oelkrug, D.; Uhl, L.; Wilkinson, F.; Willsher, C. J. *J. Phys. Chem.* **1989**, *93*, 4551.
- (16) Oelkrug, D.; Radjaipoar, M. *Zeit. Physik. Chemie New Folge* **1980**, *123*, 163.
- (17) McLaughlin, W. L.; Humphreys, J. C.; Radak, B. B.; Miller, A.; Olejnik, T. A.; *Radiat. Phys. Chem.* **1979**, *14*, 535. McLaughlin, W. L.; Boyd, A. W.; Chadwick K. H.; McDonald, J. C.; Miller, A. In *Dosimetry for radiation processing*; Taylor and Frances: London, 1989; Chapter 8.
- (18) Choi, H. T.; Haglund, J. A.; Lipsky, S. J. *J. Phys. Chem.* **1983**, *87*, 1583. Mozumder, A. *Fundamentals of Radiation Chemistry*; Academic Press: New York, 1999.
- (19) Asmus, K.-D.; Fendler, J. H. *J. Phys. Chem.* **1968**, *72*, 4285.
- (20) Zhang, G.; Thomas, J. K. *J. Phys. Chem.* **1994**, *98*, 11714.
- (21) Milosavljevic, B. H.; Thomas, J. K. *Radiat. Phys. Chem.* **2001**, *62*, 3.
- (22) Tanimura, K.; Tanaka, T.; Itoh, N. *Phys. Rev. Lett.* **1983**, *51*, 423. Tanimura, K.; Itoh, C.; Itoh, N. *J. Phys. C* **1988**, *21*, 1869. Itoh, C.; Tanimura, K.; Itoh, N. *J. Phys. C* **1988**, *21*, 4693. Itoh, C.; Suzuki, T.; Itoh, N. *Phys. Rev. B* **1990**, *41*, 3794.
- (23) Saeta, P. N.; Greene, B. I. *Phys. Rev. Lett.* **1993**, *70*, 3588. Audebert, P.; Daguzan, P.; Dos Santos, A.; Gauthier, J. C.; Geindre, J. P.; Guizard, S.; Hamoniaux, G.; Krastev, K.; Martin, P.; Petite, G.; Antonetti, A. *Phys. Rev. Lett.* **1994**, *73*, 1990.